HHS Public Access

Author manuscript

Chem Res Toxicol. Author manuscript; available in PMC 2017 June 01.

Published in final edited form as:

Chem Res Toxicol. 2014 July 21; 27(7): 1155–1165. doi:10.1021/tx500032e.

MITOCHONDRIA TARGETED SPIN TRAPS: SYNTHESIS, SUPEROXIDE SPIN TRAPPING AND MITOCHONDRIAL UPTAKE

Micael Hardy[††], **Florent Poulhés**[††], **Egon Rizzato**[††], **Antal Rockenbauer**[‡‡], **Karol Banaszak**[††], **Hakim Karoui**[††], **Marcos Lopez**[◦], **Jacek Zielonka**[†,‡], **Jeannette Vasquez-Vivar**[†,‡], **Savitha Sethumadhavan**[†,‡], **Balaraman Kalyanaraman**[†,‡], **Paul Tordo**[*,††], and **Olivier Ouari**[*,††]

[††]Aix Marseille Université, CNRS, ICR UMR 7273, 13397 Marseille, France

[†]Department of Biophysics, Medical College of Wisconsin, Milwaukee, WI 53226, USA

[‡]Free Radical Research Center, Medical College of Wisconsin, Milwaukee, WI 53226, USA

[‡‡]Institute for Molecular Pharmacology, Research Center for Natural Sciences, Hungarian Academy of Sciences, 1525 Budapest, PO Box 17, Hungary

[◦]Centro Tecnologico Empresarial, Cra 5a No. 6-33, Floridablanca, Colombia

Abstract

Development of reliable methods and site-specific detection of free radicals is an active area of research. Here, we describe the synthesis and radical-trapping properties of new derivatives of DEPMPO and DIPMPO, bearing mitochondria-targeting triphenylphosphonium cationic moiety or guanidinium cationic group. All the spin traps prepared have been observed to efficiently trap superoxide radical anion in cell-free system. The superoxide spin adducts exhibited similar spectral properties indicating no significant differences in the geometry of the cyclic nitroxide moieties of the spin adducts. The superoxide adduct stability was measured and observed to be highest ($t_{1/2}$ = 73 min) for DIPPMPO nitrone linked to triphenylphosphonium moiety via a short carbon chain (Mito-DIPPMPO). The experimental results and DFT quantum chemical calculations indicate that the cationic property of the triphenylphosphonium group may be responsible for increased superoxide trapping efficiency and adduct stability of Mito-DIPPMPO, as compared to DIPPMPO spin trap. The studies of uptake of the synthesized traps into isolated mitochondria indicated the importance of both cationic and lipophilic properties, with the DEPMPO nitrone linked to triphenylphosphonium moiety via a long carbon chain ($Mito_{10}$-DEPMPO) exhibiting the highest mitochondrial uptake. We conclude that of the synthesized traps, Mito-DIPPMPO and $Mito_{10}$-DEPMPO are the best candidates as the potential mitochondria-specific spin traps for use in biologically-relevant systems.

To whom correspondence should be addressed: O. Ouari, P. Tordo, Aix-Marseille Université, CNRS, ICR UMR 7273, SREP, Centre de Saint Jérôme, 13397. olivier.ouari@univ-amu.fr; paul.tordo@univ-amu.fr.

The authors declare no competing financial interest.

Supporting information

^{1}H, ^{31}P, ^{13}C NMR and EPR spectra, X-Ray data and Quantum-Mechanical calculations. This information is available free of charge via the Internet at http://pubs.acs.org/.

Graphical Abstract

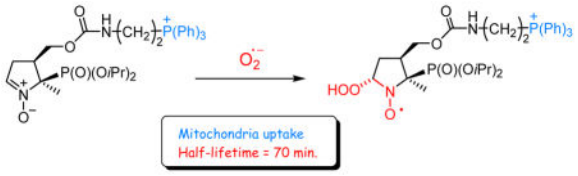

Keywords

Superoxide free radical; Electron paramagnetic resonance (EPR); Spin-trapping; Mitochondria targeting; DEPMPO; ROS

Introduction

There is increased evidence for the involvement of superoxide radical anion ($O_2^{\bullet-}$) in cell damage and disease *via* direct effects or through formation of secondary reactive oxygen and nitrogen species (ROS, RNS).[1–3] The role of these species in the pathogenesis and progression of diseases such as atherosclerosis,[4] diabetes,[5] cancer,[6] neurodegenerative diseases,[7,8] is however supported by indirect evidence due to the difficulties of direct detection of ROS and RNS in vivo. To gain information on the mechanisms controlling ROS production at the molecular level, the development of new reliable and efficient techniques for their detection[9,10] is needed. Mechanistic studies on the role of $O_2^{\bullet-}$ in oxidative stress processes is made particularly difficult by its low steady state concentration and the lack of highly specific probes that allow its unequivocal identification and quantification. Electron paramagnetic resonance (EPR) in combination with the spin trapping technique is the method of choice to detect and characterize radicals such as $O_2^{\bullet-}$.[11–15] In the spin trapping technique, a spin trap, typically a nitrone or nitroso probe, is introduced into the system under investigation to scavenge radicals which are too short-lived to be directly detected by EPR. The EPR spectra of the resulting persistent nitroxide spin adducts can usually be recorded and the spectral analysis can bring valuable information on the chemical identity and dynamics of the radical species produced in the investigated system. However, different drawbacks still limit the use and reliability of the spin trapping for in cell and *in vivo* studies, and its application to the characterization of $O_2^{\bullet-}$ and other oxygen-centered radicals still needs to be improved. Important progress has been made over the last years, notably with the development of new spin traps that form superoxide spin adducts exhibiting half-life times significantly longer (17 to 45 min)[16–20] than that observed for the most widely used nitrone spin trap, DMPO (~1 min).[21–23] Recent research in the oxidative stress field has focused on the development of targeted probes for detecting reactive species in cells.[24,25] Oxygen can be partially reduced by mitochondrial electron transfer protein complexes I and III to $O_2^{\bullet-}$ leading to cell dysfunction.[26,27] Therefore, targeting spin traps to mitochondria might help to characterize the contribution of mitochondrial $O_2^{\bullet-}$. Lipophilic cations such as triphenylphosphonium (TPP^+) and N-alkylpyridinium ions have been shown to be effective mitochondria targeting agents. Their uptake across the mitochondrial inner membrane is enhanced by the mitochondrial membrane potential ($\Delta\Psi$) according to Nernst equation, with a predicted ~10-fold accumulation of the cation within

mitochondria for every ~60 mV increase in $\Delta\Psi$.[26,28,29] In the recent years, TPP^+-conjugated probes have been used in numerous studies focused on mitochondria-associated responses. For instance, Murphy et al.[30] have determined that MitoQ, a TPP^+-conjugated ubiquinone antioxidant, accumulates up to several hundred-fold in mitochondria matrix and selectively protected mitochondria, both *in vitro* and *in vivo* from the oxidative damage.[31] Mitochondria-targeted cyclic- and linear nitrones have been studied but usually these reagents have limited spin trapping properties.[29,32,33] Recently, we reported the synthesis and the spin trapping properties of the TPP^+-conjugated DEPMPO spin trap (Mito-DEPMPO).[16,34] Using this new reagent, we demonstrated that the detection of superoxide radical anion generated from intact isolated mitochondria is feasible. This result can be explained by the accumulation of Mito-DEPMPO in mitochondria, but we have also shown that compared with DEPMPO, the rate of trapping of superoxide with Mito-DEPMPO is about two times higher, and that the half-life of the $O_2^{\bullet-}$ adduct is about 2.5 times longer. However, the reasons for these differences between DEPMPO and Mito-DEPMPO are not clear and we speculated that electrostatic interactions between the TPP^+ cation and the $O_2^{\bullet-}$ or / and the presence of stabilizing H-bonds in the $O_2^{\bullet-}$ adduct might contribute to the observed improvement in superoxide-trapping properties of Mito-DEPMPO.

To better understand the spin trapping properties of mitochondria-targeted nitrones and to optimize the influence of the TPP^+ cation on the spin trapping of $O_2^{\bullet-}$, we have synthesized a series of Mito-DEPMPO analogues **6**–**12** (Scheme 1). In the series Mito-DIPPMPO **6**, $Mito_5$-DIPPMPO **7** and $Mito_{10}$-DEPMPO **9,** the length of the linker (C4-$CH_2OC(O)NH(CH_2)_n$-TPP^+) between the C4 and the TPP^+ moiety increases (n = 2, 5 and 10 respectively). Two TPP^+ moieties are present in Mito-bis-DIPPMPO **8** (n = 2) and a neutral -$N(H)CPh_3$ group mimicking the lipophilicity of TPP^+ was introduced in TritA-DEPMPO **10** (n = 2), finally the TPP^+ cation was replaced by a guanidium group in Gua-DIPPMPO **11** and Agm-DIPPMPO **12** (n = 2 and 4 respectively).

NHS-DIPPMPO and NHS-DEPMPO were used as precursors for the synthesis of the series of derivatives, illustrating the versatility of the post-functionalization step (Scheme 2). For synthetic convenience, NHS-DIPPMPO was mostly used.

Hereafter we describe the synthesis of compounds **6**–**12**, their spin trapping properties and the binding/uptake properties of compounds **6**–**10** to energized mitochondria.

Results and Discussion

Synthesis

NHS-DIPPMPO **5** was prepared (32% overall yield) in a four-step synthetic sequence (Scheme 2) following the procedure described by Hardy et al.[16] (SI).

Nitrofuranone **2** was obtained in 74% yield by reacting nitrophosphonate **1** with 2(5H)-furanone in the presence of tributylphosphine as catalyst. Reduction of **2** by DIBAL-H at -78°C led to hemiacetal **3** in good yield (75%). Reductive cyclization of nitroaldehyde **3** in the presence of zinc and ammonium chloride afforded nitrones **4** and **4′** as a mixture of *cis* / *trans* diastereoisomers, which were separated on silicagel column chromatography (60%

yield for **4**). Compound **4** was recrystallized in Et_2O / Pentane (8:2) and the geometry obtained by X-ray diffraction confirmed the *cis* position of the di-isopropylphosphonyl group relative to the hydroxymethylene moiety (Figure 1).

Reaction of diastereoisomer **4** with N,N′-disuccinimidylcarbonate (DSC) in the presence of triethylamine afforded NHS-DIPPMPO **5** in 95% yield.

Compounds **6**–**12** were obtained by reacting NHS-DIPPMPO or NHS-DEPMPO with the amino function of the appropriate side chain, with yields ranging from 50 to 91% (Scheme 3 and SI).

Except TritA-DIPPMPO **10** and $Mito_{10}$-DEPMPO **9**, all compounds were soluble up to 50 mM concentration in water and in phosphate buffer solutions.

EPR / spin trapping

EPR / spin trapping of superoxide—The $O_2^{\bullet-}$ trapping properties (Scheme 4) of compounds **6**–**12** were evaluated using two different $O_2^{\bullet-}$ generating systems: hypoxanthine/xanthine oxidase (HX/XO) and KO_2/18-crown-6-ether/DMSO (KO_2/CE/DMSO) in phosphate buffer. Figure 2 shows the EPR spectra obtained after 10 min incubation of a mixture containing HX (0.4 mM), XO (0.04 U mL^{-1}), DTPA (1 mM) and the spin trap (20 mM of Mito-DIPPMPO; **8** Mito-bis-DIPPMPO; **7** $Mito_5$-DIPPMPO and **9** $Mito_{10}$-DEPMPO) in oxygen-bubbled phosphate buffer (0.1 M, pH 7.3). The computer calculated EPR spectra, obtained using the parameters reported in Table 1, are shown as gray lines (Figure 2).

In the presence of superoxide dismutase (SOD), no EPR signal was detected (Figure 2, b, d, f, h). Furthermore, for compounds **6**–**9**, identical EPR signals were observed using either the HX/XO or the (KO_2/CE/DMSO) system, the signals being particularly long-lasting with the former. After 30 minutes, a weak additional signal (< 10%) is observable and was assigned to the HO-adduct. These results establish that the EPR signals shown in Figure 2 can be unambiguously assigned to the corresponding $O_2^{\bullet-}$ spin adducts.

All spectra appear as doublet (^{31}P coupling) of significantly distorted quartets resulting from close couplings with the ^{14}N and $^1H_{\beta,}$ they were calculated (Table 1) using the EPR/ROKI program.[35] For all the series the best fit was obtained assuming both that the spin trapping reaction yields only the trans-diastereoisomer (-OOH and -P(O)$(OR)_2$ groups in a trans geometry) and secondly the existence of a chemical exchange between two conformational sites T_1 and T_2 composed of rapidly exchanging conformers. In the case of the DEPMPO-OOH and DIPPMPO-OOH spin adducts, the same assumptions were made to account for the dramatic alternate line-width observed on the spectra of the trans-diastereoisomers.[34–38]

Using guanidine salts as inhibitors of XO enzyme,[39] and Agm-DIPPMPO **11** and Gua-DIPPMPO **12** no signals were observed in incubations with HX/XO system. Incubations with KO_2/CE/DMSO led to detection of very similar EPR signals to Mito-DIPPMPO-OOH (Figure 3), confirming the ability of the probes to trap $O_2^{\bullet-}$ and consistent with the inhibitory effects of spin traps **11** and **12** on the XO activity.

Within the series of superoxide adduct of compounds **6**–**12**, the values of the determined EPR parameters are similar and close to the values obtained previously for Mito-DEPMPO-OOH (Table 1), suggesting that the modification of the C4 side-chain does not change significantly the geometry of the preferred conformers of these spin adducts. However, as it is shown below the C4 side chain has a strong influence on their stability.

Decay kinetics of superoxide adduct—Once the concentration of the $O_2^{\bullet -}$ spin adduct has reached a plateau (after ~ 9 min), the further formation of $O_2^{\bullet -}$ spin adduct was stopped by the addition of a large amount of SOD and the decay kinetics of the $O_2^{\bullet -}$ adduct was monitored by following the changes in EPR signal intensity. The kinetic studies were performed at 23°C in 50 μL capillaries, setting the microwave power of the EPR spectrometer at 20 mW. The signal decay was monitored during 70 min. recording successive spectra every 42 s (Figure 4). All the recorded spectra were simulated using the Rocky program.[35] The decay curves for the superoxide spin adducts of **6**–**9** are shown in SI and the apparent half-life times are listed in Table 2. It is worth noting that the half-lifetime values depend strongly on the experimental conditions and various parameters such as temperature, microwave power, EPR cell (capillaries, AquaX cell) must be carefully controlled in order to get reproducible results.

The values of apparent half-lifetime ($t_{1/2}$) for the superoxide-adducts are reported in Table 2.

As one might expected given the results obtained with Mito-DEPMPO, [16] a ratio of 2.6 was found between the apparent half-life time of Mito-DIPPMPO-OOH (n = 2) and that observed with the parent nitrone DIPPMPO-OOH (this ratio amounts to 2.4 – 2.5, in the case of Mito-DEPMPO-OOH and DEPMPO-OOH). However, when the spacer arm linking the TPP^+ group and the pyrroline ring was made longer (**7**, $Mito_5$-DIPPMPO and **9**, $Mito_{10}$-DEPMPO) and when two triphenyphosphonium groups are appended (**8**, Mito-bis-DIPPMPO), the stability of the corresponding superoxide adducts is very close to that observed for the parent nitrone spin adducts. For Agm-DIPPMPO and Gua-DIPPMPO, attempts to perform a kinetic study using the KO_2/CE/DMSO system were frustrated due to the poor reproducibility of the procedure, in addition to decreased persistency of the $O_2^{\bullet -}$ adducts. Measures of TritA-DEPMPO-OOH (**10**) half-lifetime was not possible because of low solubility of TritA-DEPMPO.

EPR characterization of hydroxyl and 1-hydroxyethyl radicals

Hydroxyl radical—When a Fenton system was used in phosphate buffer to generate $HO^{\bullet}$ in the presence of compounds **6**–**9**, complex signals of low intensity corresponding to the superimposition of the spectra of different spin adducts were observed (data not shown). These signals are diminished in intensity in the presence of catalase, indicating that these signals depend on hydrogen peroxide breakdown. A twelve line EPR spectra corresponding to the $HO^{\bullet}$ adducts of **6, 8** and **9** (Figure 5) were obtained by reduction of the corresponding superoxide adducts with glutathione peroxidase / glutathione (GPx/GSH), the hyperfine coupling constants are listed in Table 3.

Quantum-Mechanical calculations—Under the experimental conditions we used for our spin trapping experiments, the apparent half life time of Mito-DIPPMPO-OOH is the longest ever observed for the superoxide spin adduct of a spin trap belonging to the pyrroline *N*-oxide series. In an attempt to rationalize this result, we undertook a Density Functional Theory (DFT) approach to the structure of Mito-DIPPMPO (**6**) and Mito-DIPPMPO-OOH (**6**-OOH).

The structures of four conformers ($\mathbf{6}_A$ to $\mathbf{6}_D$, see SI) have been obtained for **6** and one of lower energy ($\mathbf{6}_A$) is shown in Figure 7. For all the calculated conformers, the geometry of the pyrroline ring and its two C5 substituents are almost the same and very close to that determined by X-ray diffraction for compound **4** (Figure 1). This geometry is characterized by an envelope at C4 and a pseudo-axial (iPrO)$_2$P(O)- substituent with its P=O bond directed towards the pyrroline ring. The five calculated conformers differ by the geometry of the C4 substituent. For conformer $\mathbf{6}_A$, the geometry of the (iPrO)$_2$P(O)- and C4 substituents is in agreement with the trans addition of superoxide leading to the observed trans-diastereoisomer spin adduct. Furthermore the kinetic of addition should benefit from the electrostatic interaction of $O_2^{-\bullet}$ with the positive charges brought by the TPP^+ moiety, and we indeed observed that it increases by a factor 2 compared with DIPPMPO.

The structures of four conformers **6**-OOH_A to **6**-OOH_D (Figure 7 and SI) have been obtained for the superoxide adduct of DIPPMPO. The conformers **6**-$OOH_{A,B,C}$ correspond to the trans addition of superoxide to **6,** and their energies are very close (ΔE_{max} = 2.93 kJ.mole^{-1}). For these three conformers the positively charged phosphorus atom P8 is close to the hydroperoxyl group (P_8-O_{10} = 4.94 Å for **6**-OOH_A, Figure 7) and stabilizing interactions can be established between the positive hydrogen atoms (d = + 0.31, Mulliken charge) of one phenyl group and the oxygen lone pairs (H_9-O_{10} = 2.51 Å for **6**-OOH_A, Figure 7). These interactions of the TPP^+ moiety with the hydroperoxyl group likely contribute to the stabilization of the species, resulting in the especially long half-life time observed. For conformer **6**-OOH_D, the distance P_8-O_{10} is much higher (10.53 Å) and its energy is 6.10 to 9.02 kJ.mole^{-1} higher compared to conformers **6**-$OOH_{A,B,C}$. For these later conformers the agreement between the calculated and the experimental hyperfine coupling constants is satisfying [for **6**-OOH_A, the lowest energy conformer, A_N = 1.00 mT $(1.28)_{exp}$; A_P = 5.00 mT $(5.27)_{exp}$; $A_{H\beta}$ = 1.13 mT $(1.17)_{exp}$].

Mitochondrial uptake studies

The mitochondrial binding/uptake of compounds **6–10** was evaluated from the decrease of the compounds' concentration after incubation during 30 minutes with respiring mitochondria. No kinetic study was performed and the method was based on the quantification of the compounds remaining in the supernatant (see Experimental Section). The results of mitochondrial uptake experiments are reported in Table 4 represent the percentage of decrease in compounds' concentration during incubation with energized (with succinate) mitochondria, as compared to mitochondria without succinate. The effects of triphenylphosphonium (TPP^+) in improving their affinity for mitochondria is clear from the investigated series, where little effects are seen for DIPPMPO and no membrane potential-dependent uptake is observed for TritA-DEPMPO **10**. We conclude that highly delocalized

cationic charge on the lipophilic phenyl rings is necessary for the accumulation in mitochondria in membrane potential –dependent manner. Surprisingly, the presence of two TPP^+ in Mito-bis-DIPPMPO **8** did not increase the uptake, may be due to the close vicinity of the two moieties.[40] The best uptake was obtained with $Mito_{10}$-DEPMPO **9**, probably due its higher hydrophobicity and amphiphilic properties. The mitochondrial uptake of $Mito_{10}$-DEPMPO **9** and Mito-bis-DIPPMPO **8** has been independently confirmed by LC-MS/MS analysis of the extracts of mitochondrial pellets, indicating significantly higher accumulation of compounds **8** and **9**, as compared to non-targeted spin trap, DIPPMPO (data not shown).

Conclusions

With the aim to develop tools for the study of $O_2^{\bullet-}$ formation in mitochondria, we have prepared a series of DIPPMPO and DEPMPO derivatives, with a substituent in the 4-position of the pyrroline ring, having different lengths and bearing a TPP^+ cation or a guanidinium group as chain end. We have studied the spin trapping properties of these new spin traps and determined their mitochondria uptake. All the compounds bearing a TPP^+ cation efficiently react with $O_2^{\bullet-}$ forming stable adducts. The results of quantum-mechanical calculations suggest that the addition of the negatively charged $O_2^{\bullet-}$ to Mito-DIPPMPO could be facilitated by the attraction exerted by the TPP^+ group. Moreover, in the most stable conformers of Mito-DIPPMPO-OOH, the interactions of the TPP^+ moiety with the hydroperoxyl group likely contribute to the stabilization of the species, resulting in the especially long half-life time observed.

Results from the mitochondria uptake studies showed the key role of the TPP^+ moiety in the targeting properties. It should be noted, however, that other factors such as the accessibility of the TPP^+ group or the amphiphilic properties of the molecule can modulate the mitochondria uptake, which cannot readily be predicted and experimental determination is required. Spin traps that can be compartmentalized or localized at particular biological sites are part of the toolbox required for maximizing the amount of useful information, as it is now clear that data obtained from multiple techniques is often required to obtain a definitive picture on the formation and role of free radicals in biological systems. The apparent half-life time of the $O_2^{\bullet-}$ adduct and the mitochondrial uptake are 73 min and 30 % for Mito-DIPPMPO (**6**), and 22 min. and 60 % for $Mito_{10}$-DEPMPO (**9**), making these new spin traps suitable candidates for mitochondrial superoxide trapping.

Experimental Section

Materials

CH_2Cl_2 was distilled under dry argon atmosphere in the presence of P_2O_5. All reagents were used as received without further purification. The reactions were monitored by TLC on silica gel and by ^{31}P NMR. Crude materials were purified by flash chromatography on Silica gel 60 (0.040–0.063 mm). ^{31}P NMR, ^{1}H NMR and ^{13}C NMR spectra were recorded with a 300 or 400 spectrometers at 121.49, 300.13 and 75.54 MHz respectively. ^{31}P NMR was taken in $CDCl_3$ using 85% H_3PO_4 as an external standard with broad-band ^{1}H decoupling. ^{1}H NMR and ^{13}C NMR were taken in $CDCl_3$ using TMS or $CDCl_3$ as internal reference respectively. Chemical shifts (δ) are reported in ppm and coupling constant *J* values in Hertz. The

assignments of NMR signals were facilitated by use of the DEPT 135 sequence for all the nitrones. High resolution MS experiments (HRMS) were performed with a mass spectrometer equipped with an electrospray ionization source operated in the positive ion mode. In this hybrid instrument, ions were measured using an orthogonal acceleration time-of-flight (oa-TOF) mass analyzer.

Synthesis of the nitrone NHS-DIPPMPO 5—The synthesis was performed adapting the procedure described by Hardy et al.[41] The nitrophosphonate **1** has already been described.[42]

4-(1-Diisopropyloxyphosphoryl-1-nitroethyl)-tetrahydrofuran-2-one 2: The product **2** was obtained as a yellow oil (25 g, 74 %) corresponding to a mixture of two diastereoisomers. ^{31}P NMR (121.49 MHz) δ 12.84 (60%), 12.95 (40%); ^{1}H NMR (300.13 MHz) δ 1.40–1.30 (12H, m), 1.75 (3H, d, *J* = 14.4), 2.74–2.36 (2H, m), 3.82–3.63 (1H, m), 4.54–4.07 (2H, m), 4.86–4.66 (2H, m).^{13}C NMR (75.47 MHz) δ 174.7 (C^{IV}, s), 174.6 (C^{IV}, s), 90.5 (C^{IV}, d, *J* = 148.0), 90.2 (d, *J* = 147.1), 74.4 (s), 74.3 (s), 74.2 (d, *J* = 1.8), 74.0 (d, *J* = 1.4), 68.4 (d, *J* = 2.8), 68.2 (s), 40.2 (s), 39.7 (s), 30.3 (d, *J* = 2.8), 29.9 (d, *J* = 8.3), 24.1 (d, *J* = 3.2), 23.9 (d, *J* = 1.8), 23.8 (d, *J* = 1.8), 23.5 (d, *J* = 1.4), 23.4 (s), 23.3 (d, *J* = 1.4), 16.2 (d, *J* = 1.4), 16.1 (d, *J* = 1.4). HMRS calcd. for $C_{12}H_{22}NO_7P$; $[C_{12}H_{22}NO_7P+NH_4]^+$; 341.1472, found: 341.1474.

4-(1-Diisopropyloxyphosphoryl-1-nitroethyl)-2-hydroxytetrahydrofurane 3: The product **3** was obtained as a yellow oil (3 g, 75%) corresponding to a mixture of four diastereoisomers. ^{31}P NMR (121.49 MHz) δ14.58 (44%), 14.75 (22%), 14.95 (34%); ^{1}H NMR (300.13 MHz) δ 1.40–1.25 (12H, m), 1.66&1.78&1.83 (3H, 3d, *J* = 14.4, 14.5, 14,0), 1.98–1.87 (1H, m), 3.57–3.32 (1H, m), 3.94–3.60 (2H, m), 4.21–4.01 (1H, m), 4.85–4.62 (2H, m), 5.51 (1H, t, *J* = 3.2); ^{13}C NMR (75.47 MHz) δ 97.8 (s), 97.7 (s), 91.4 (C^{IV}, d, *J* = 148.4), 73.8 (d, *J* = 6.7), 73.7 (d, *J* = 6.7), 73.5 (d, *J* = 7.3), 67.1 (d, *J* = 0.9), 66.9 (d, *J* = 0.9), 43.0 (s), 42.3 (s), 35.2, (s), 34.9 (s), 34.8 (s), 24.2 (d, *J* = 7.8), 24.5 (d, *J* = 5.0), 24.4 (d, *J* = 5.9), 15.2 (s), 14.9 (s). HMRS calcd. for $C_{12}H_{24}NO_7P$; $[C_{12}H_{22}NO_7P+H]^+$; 326.1363, found: 326.1363.

5-Diisopropyloxyphosphoryl-5-methyl-4-hydroxymethyl-1-pyrroline *N*-Oxide 4 and 4′: The nitrones **4** and **4′** were obtained in 60% yield (7 g) corresponding to a mixture of 2 diastereoisomers. (4R*, 5R*)-4-HMDIPPMPO **4**; ^{31}P NMR (121.49 MHz) δ 21.19; ^{1}H NMR (300.13 MHz) δ 1.31 (3H, d, *J* = 6.2), 1.32 (3H, d, *J* = 6.0), 1.37 (3H, d, *J* = 6.2), 1.41 (3H, d, *J* = 6.2), 1.70 (3H, d, *J* = 14.5), 2.75–2.37 (3H, m), 3.92–3.82 (2H, m), 4.18 (1H, m), 4.95–4.71 (2H, m), 6.88 (1H, dt, *J* = 2.4, 2.4); ^{13}C NMR (75.47 MHz) δ 134.1 (1C, d, *J* = 7.7), 77.0 (1C, d, *J* = 152.0), 73.3 (1C, d, *J* = 7.1), 72.8 (1C, d, *J* = 7.7), 62.4 (1C, d, *J* = 5.5), 49.3 (1C, d, *J* = 5.7), 29.2 (1C, s), 24.2 (1C, d, *J* = 2.7), 24.0 (1C, d, *J* = 2.7), 24.8 (1C, d, *J* = 6.0), 23.6 (1C, d, *J* = 5.5), 21.4 (1C, d, *J* = 1.6); ESI-MS : m/z : 293 $[M + H]^+$. HMRS calcd. for $C_{12}H_{24}NO_5P$; $[C_{12}H_{25}NO_5P+H]^+$; 294.1465, found: 294.1465.

(4S*,5R*)-4-HMDIPPMPO **4′** ^{31}P NMR (121.49 MHz) δ 21.97; ^{1}H NMR (300.13 MHz) δ 1.31&1.32 (12H, 2d, *J* = 6.2, 6.2), 1.57 (3H, d, *J* = 16.0), 2.60–2.34 (2H, m), 3.14–2.72 (2H, m), 3.79–3.69 (1H, m), 4.2–3.90 (1H, m), 4.90–4.67 (2H, m), 6.82 (1H, dt, *J* = 2.7, 2.6); ^{13}C

NMR (75.47 MHz) δ 134.2 (1C, d, *J* = 8.8), 76.7 (1C, d, *J* = 159.7), 73.0 (1C, d, *J* = 7.1), 72.1 (1C, d, *J* = 7.7), 61.4 (1C, d, *J* = 6.0), 40.9 (1C, s), 30.0 (1C, d, *J* = 4.9), 24.2 (1C, d, *J* = 2.7), 23.9 (1C, d, *J* = 4.4), 23.8 (1C, d, *J* = 4.9), 23.5 (1C, d, *J* = 6.6), 14.2 (1C, s).

(4R*,5R*)-5-diisopropyloxyphosphoryl-5-methyl-4-(succinimidyloxycarbonyloxymethyl)-1-pyrroline *N*-Oxide 5: The nitrone NHS-DIPPMPO **5** was obtained as a white crystal (1.4 g, 100%); ^{31}P NMR (81.01 MHz):δ 18.0; ^{1}H NMR (300.13 MHz) δ 1.41–1.26 (12H, m), 1.66 (3H, d, *J* = 14.0), 2.90–2.63 (3H, m), 2.8 (4H, s), 4.63–4.48 (1H, m), 4.86–4.67 (3H, m), 6.92 (1H, m); ^{13}C NMR (50.32 MHz) δ 168.5 (2C, s), 151.3 (1C, s), 133.5 (1C, d, *J* = 7.3), 75.9 (1C, d, *J* = 149.8), 73.9 (1C, d, *J* = 6.4), 72.1 (1C, d, *J* = 7.8), 70.5 (1C, d, *J* = 3.2), 45.6 (1C, d, *J* = 2.3), 30.0 (1C, d, *J* = 0.9), 25.4 (2C, s), 24.5 (1C, d, *J* = 1.4), 23.8 (1C, d, *J* = 1.4), 23.7 (1C, d, *J* = 1.8), 23.4 (1C, d, *J* = 7.3), 20.3 (1C, s). HMRS calcd. for $C_{17}H_{27}N_2O_9P$; $[C_{17}H_{27}N_2O_9P + H]^+$; 435.1527, found: 435.1527.

Synthesis of the nitrone Mito-DIPPMPO 6

Mito-DIPPMPO 6: To a mixture of NHS-DIPPMPO (0.2 g, 0.46 mmol) and (2-aminoethyl) triphenylphosphonium Bromide (0.18 g, 0.46 mmol) in CH_2Cl_2 (15 mL) was added at room temperature under inert atmosphere triethylamine (141 μL, 1.06 mmol). The reaction mixture was stirred for 3 h. The solution was washed with 8 ml of distilled water, and extracted 3 times with $CHCl_3$. The organic layers were dried over Na_2SO_4 and the solvent distilled under reduced pressure. Purification of the crude product by flash chromatography on silicagel (CH_2Cl_2/EtOH 80:20) afforded a white powder (0.28 g, 86 %), corresponding to Mito-DIPPMPO **6**. ^{31}P NMR (121.49 MHz) δ 17.8, 20.9; ^{1}H NMR (300.13 MHz) δ 1.38–1.27 (12H, m), 1.62 (3H, d, *J* = 14.1), 2.68–2.52 (3H, broad band), 3.57–3.68 (2H, m), 3.95–3.33 (2H, m), 4.17–4.07 (1H, m), 4.36–4.29 (1H, m), 4.79–4.67 (2H, m), 6.91 (1H, m), 7.52 (1H, t, *J* = 6.0), 7.82–7.63 (15H, broad band); ^{13}C NMR (75.47 MHz) δ 156.5 (1C, s), 135.2 (3C, d, *J* = 2.9), 134.6 (1C, d, *J* = 7.3), 133.6 (6C, d, *J* = 10.3), 130.5 (6C, d, *J* = 12.4), 117.5 (3C, d, *J* = 86.5), 75.1 (1C, d, *J* = 149.6), 73.4 (1C, d, *J* = 6.6), 71.8 (1C, d, *J* = 8.0), 64.5 (1C, s), 46.4 (1C, d, *J* = 2.2), 35.2 (1C, s), 30.7 (1C, s), 24.5 (1C, d, *J* = 1.5), 24.0 (1C, d, *J* = 3.7), 25.8 (1C, d, *J* = 5.1), 23.6 (1C, d, *J* = 7.3), 23.3 (1C d, *J* = 48.4), 20.3 (1C, s). HMRS calcd. for $[C_{33}H_{43}N_2O_6P_2]^+$, Br^-; $[C_{33}H_{43}N_2O_6P_2]^+$ 625.2591, found: 625.2587.

Synthesis of the nitrone Mito-bis-DIPPMPO 8

Bis-[2-(triphenylphosphonium bromide)-ethyl]-amine A: A mixture containing Bis-(2-bromo-ethyl)-amine[43] (7 g, 0.03 mol) and triphenylphosphane (16 g, 0.061 mol) in acetonitrile (50 mL) was refluxed for 48 hours. The solvent distilled under reduced pressure. Purification of the crude product by flash chromatography on a silicagel (CH_2Cl_2/EtOH 80:20) afforded a brown solid **A** (12 g, 52%).^{31}P NMR (121.49 MHz) 23.56, ^{1}H NMR (300.13 MHz) δ 3.06–3.12 (4H, m), 3.72–3.80 (4H, m), 7.60–7.82 (30H, m); ^{13}C NMR (75.47 MHz) δ 134.6 (6C, d, *J* = 2.9), 133.8 (12C, d, *J* = 10.3), 130.4 (12C, d, *J* = 12.5), 118.5 (6C, d, *J* = 86.6), 41.7 (2C, s), 23.7 (2C, d, *J* = 50.6). ESI-MS : m/z : 297.6 $[M + H]^{++}$.

Mito-bis-DIPPMPO 8: To a mixture of NHS-DIPPMPO (0.2 g, 0.46 mmol) and Bis-[2-(triphenylphosphonium bromide)-ethyl]-amine **A** (0.37 g, 0.46 mmol) in CH_2Cl_2 (5 mL)

was added at room temperature under inert atmosphere triethylamine (141 μL, 1.06 mmol). The reaction mixture was stirred for 3 h. The solution was washed with 8 ml of distilled water, and extracted 3 times with $CHCl_3$. The organic layers were combined and dried over Na_2SO_4 and the solvent removed under reduce pressure. Purification of the crude product by flash chromatography on silicagel (CH_2Cl_2/EtOH 80:20) afforded a white powder (0.25 g, 50 %), corresponding to Mito-bis-DIPPMPO **8**. ^{31}P NMR (121.49 MHz) 17.61, 21.89; ^{1}H NMR (300.13 MHz) δ 1.38–1.26 (12H, m), 1.53 (3H, d, *J* = 13.8), 2.82–2.62 (3H, m), 4.10–3.90 (4H, m), 4.35–4.12 (4H, m), 4.60–4.39 (2H, m), 4.79–4.62 (2H, m), 6.83 (1H, m), 7.60–7.98 (30H, m); ^{13}C NMR (75.47 MHz) δ 154.9 (1C, s), 134.8 (3C, d, *J* = 2.9), 134.7 (3C, d, *J* = 2.9), 134.6 (1C, d, *J* = 8.8), 134.2 (6C, d, *J* = 7.3), 134.1 (6C, d, *J* = 7.3), 130.4 (6C, d, *J* = 12.5), 130.3 (6C, d, *J* = 12.5), 117.9 (3C, d, *J* = 86.6), 117.8 (3C, d, *J* = 86.8), 75.8 (1C, d, *J* = 149.6), 73.5 (1C, d, *J* = 6.6), 71.7 (1C, d, *J* = 7.3), 64.3 (1C, d, *J* = 2.2), 45.8 (1C, d, *J* = 2.2), 42.9 (1C, s), 42.6 (1C, s), 29.2 (1C, s), 24.5 (1C, s), 24.0 (1C, d, *J* = 4.4), 23.9 (1C, d, *J* = 4.4), 23.4 (1C, d, *J* = 7.3), 23.1 (1C, d, *J* = 46.2), 22.1 (1C, d, *J* = 47.7), 20.3 (1C, s). HMRS calcd. for $[C_{53}H_{61}N_2O_6P_3]^{2+}$, $2Br^-$; $[C_{53}H_{61}N_2O_6P_3]^{2+}$ 457.1866, found: 457.1868.

Synthesis of the nitrone Mito$_5$-DIPPMPO 7

Mito$_5$-DIPPMPO 7: To a mixture of NHS-DIPPMPO (0.200 g, 0.46 mmol) and (2-Aminopentyl) triphenylphosphonium bromide[44] (0.190 g, 0.46 mmol) in CH_2Cl_2 (20 mL) was added at room temperature under inert atmosphere triethylamine (147 μL, 6 mmol). The reaction mixture was stirred for 3 h. The solution was washed with 8 ml of distilled water, and extracted 3 times with $CHCl_3$. The organic layers were combined and dried over Na_2SO_4 and the solvent removed under reduce pressure. Purification of the crude product by flash chromatography on silicagel (CH_2Cl_2/EtOH 80:20) afforded a white powder (0.171 g, 50 %), corresponding to Mito$_5$-DIPPMPO **7**. ^{31}P NMR (121.49 MHz) δ 18.0, 24.3; ^{1}H NMR (300.13 MHz) δ 1.38–1.26 (12H, m), 1.62 (3H, d, *J* = 14.0), 1.71–1.57 (6H, m), 2.72–2.61 (3H, broad band), 3.13–3.09 (2H, m), 3.73–3.66 (2H, m), 4.21–4.16 (1H, m), 4.45–4.40 (1H, m), 4.77–4.69 (2H, m), 6.29 (1H, t, *J* = 5.5), 6.91 (1H, m), 7.82–7.63 (15 H, broad band); ^{13}C NMR (75.47 MHz) δ 156.6 (1C, s), 135.0 (3C, d, *J* = 2.9), 135.5 (6C, d, *J* = 10.3), 130.4 (6C, d, *J* = 12.5), 118.2 (3C, d, *J* = 85.8), 75.9 (1C, d, *J* = 150.4), 73.2 (1C, d, *J* = 6.6), 71.6 (1C, d, *J* = 7.3), 64.0 (1C, s), 46.5 (1C, d, *J* = 2.2), 39.9 (1C, s), 30.7 (1C, s), 29.5 (1C, s), 28.3 (1C, s), 26.9 (1C, d, *J* = 16.7), 24.5 (1C, d, *J* = 1.5), 23.9 (1C, d, *J* = 3.7), 23.7 (1C, d, *J* = 5.4), 23.4 (1C, d, *J* = 6.6), 22.5 (1C, d, *J* = 49.9), 21.8 (1C, d, *J* = 4.4), 20.3 (1C, s). HMRS calcd. for $[C_{36}H_{49}N_2O_6P_2]^+$, Br^-; $[C_{36}H_{49}N_2O_6P_2]^+$ 667.3060, found: 667.3060.

Synthesis of the nitrone Mito$_{10}$-DEPMPO 9

(10-phtalimidodecyl) triphenylphosphonium bromide B: A mixture containing Bromophtalimide (7 g, 0.019 mol) and triphenylphosphane (5 g, 0.019 mol) in acetonitrile (60 mL) was refluxed for 15 hours. The solvent distilled under reduced pressure. Purification of the crude product by flash chromatography on a silicagel (CH_2Cl_2/EtOH 80:20) afforded a white solid **B** (9 g, 73%). MS calcd for $[C_{36}H_{39}NO_2P]^+$, Br^-; $[C_{36}H_{39}NO_2P]^+$, 548.3, found: 548.3.

(10-Aminodecyl) triphenylphosphonium Bromide C: To a solution of **B** (7 g, 0.011 mol) in EtOH (70 mL) was added hydrazine (0.54 mL, 0.011 mol). The mixture was refluxed for 15 hours. The solvent is distilled and the impurity was recrystallized using a mixture Et_2O/EtOH (2/1). The product was purified by flash chromatography on silicagel (CH_2Cl_2/EtOH 80:20) afforded a yellow solid **C** (4 g, 73%). ^{31}P NMR (121.49 MHz) δ 24.61; ^{1}H NMR (300.13 MHz) δ 7.95–7.73 (15H, m), 3.70–3.55 (2H, m), 2.80–2.70 (2H, m), 1.60–1.40 (6H, m), 1.35–1.10 (10H, m). MS calcd for $[C_{28}H_{37}NP]^+$, Br^-; $[C_{28}H_{37}NP]^+$, 418.2, found: 418.2.

$Mito_{10}$-DEPMPO 9: To a mixture of NHS-DEPMPO (0.25 g, 0.61 mmol) and (10-Aminodecyl) triphenylphosphonium bromide **C** (0.32 g, 0.62 mmol) in CH_2Cl_2 (20 mL) was added at room temperature under inert atmosphere triethylamine (0.23 mL, 1.61 mmol). The reaction mixture was stirred for 3 h, then washed with water (15 mL). The organic layer was dried over Na_2SO_4 and the solvent distilled under reduce pressure. Purification of the crude product by flash chromatography on silicagel (CH_2Cl_2/EtOH 70:30) afforded a white powder (0.31 g, 64 %), corresponding to $Mito_{10}$-DEPMPO **9**. ^{31}P NMR (121.49 MHz) δ 20.58, 25.48; ^{1}H NMR (300.13 MHz) δ 1.39–1.16 (17H, m), 1.50–1.40 (2H, m), 1.65–1.57 (3H, m), 1.68 (3H, d, *J* = 14.0), 2.80–2.55 (3H, m), 3.19–3.06 (2H, m), 3.90–3.60 (3H, m), 4.30–4.10 (5H, m), 4.56–4.45 (1H, m), 6.97 (1H, dt, *J* = 2.4, 2.4), 7.92–7.62 (15H, m); ^{13}C NMR (75.47 MHz) δ 156.1 ($1C^{IV}$, s), 134.8 (1C, d, *J* = 8.2), 134.9 (3C, d, *J* = 3), 133.7 (6C, d, *J* = 9.7), 130.4 (6C, d, *J* = 12.6), 118.5 ($3C^{IV}$, d, *J* = 85.5), 76.2 (1C, d, *J* = 155.7), 64.3 (1C, d, *J* = 6.3), 63.9 (1C, s), 62.5 (1C, d, *J* = 8.0), 46.7 (1C, d, *J* = 2.3), 41.0 (1C, s), 30.4 (1C, s), 30.2 (1C, s), 29.7 (1C, s), 29.0 (1C, s), 28.9 (2C, s), 26.52 (1C, s), 23.0 (1C, d, *J* = 49.3), 22.6 (1C, d, *J* = 4.0), 22.7 (1C, d, *J* = 49.3), 20.3 (1C, s), 16.4 (1C, d, *J* = 5.7), 16.3 (1C, d, *J* = 5.7); HRMS calcd for $[C_{39}H_{55}N_2O_6P_2]^+$, Br^-; $[C_{39}H_{55}N_2O_6P_2]^+$ 709.3530, found: 709.3529.

Synthesis of the nitrone TritA-DEPMPO 10

TritA-DEPMPO 10: To a mixture of NHS-DEPMPO (0.15 g, 3.6 mmol) and N-tritylethylenediamine hydrobromide (0.14 g, 3.6 mmol) in CH_2Cl_2 (10 mL) was added triethylamine (103 μL, 1.61 mmol) at room temperature under argon. The reaction mixture was stirred for 5 h and then washed with water (15 mL). The organic layer was dried over Na_2SO_4 and the solvent distilled under reduced pressure. Purification of the crude product by flash chromatography on a silicagel (CH_2Cl_2/EtOH 97:03) afforded a white powder (0.2 g, 91%), corresponding to TritA-DEPMPO **10**. ^{31}P NMR (121.49 MHz) δ 19.75. ^{1}H NMR (300.13 MHz) δ 7.49–7.43 (5H, m), 7.33–7.28 (4H, m), 7.27–7.20 (6H, m), 7.18 (1H, t, *J* = 1.2), 7.01 (1H, m), 5.08 (1H, t, *J* = 4.2), 4.62–4.53 (1H, m), 4.38–4.12 (5H, m), 3.37–3.21 (2H, m), 2.84–2.57 (3H, m), 2.30 (2H, t, *J* = 6.0), 1.73 (3H, d, *J* = 14.0), 1.36 (6H, dt, *J* = 7.0). ^{13}C NMR (75.47 MHz) δ 156.1 ($1C^{IV}$, s), 145.7 ($3C^{IV}$, s), 134.5 (1C, d, *J* = 8.0), 128.5 (6C, s), 127.9 (6C, s), 126.4 (3C, s), 76.1 (1C, d, *J* = 160.6), 70.6 ($1C^{IV}$, s), 64.3 (1C, d, *J* = 6.3), 64.1 (1C, s), 62.4 (1C, d, *J* = 7.4) 46.7 (1C, s), 43.6 (1C, s), 41.7 (1C, s), 30.3 (1C, s), 20.3 (1C, s), 16.3 (1C, d, *J* = 5.7), 16.2 (1C, d, *J* = 5.7). HRMS calcd for $[C_{32}H_{40}N_3O_6P]$; $[C_{32}H_{40}N_2O_6P]^+$ 594.2728, found: 594.2735.

Synthesis of the nitrone Gua-DIPPMPO 11

Gua-DIPPMPO 11: To a mixture of (2-aminoethyl)-guanidine (0.13 g, 1,1 mmol) in acetonitrile (5 mL) was added NHS-DIPPMPO **5** (0.4 g, 0.92 mmol) in 10 mL of anhydrous acetonitrile following by the addition of N-ethyldiisopropylamine (0,24 mL, 1,38 mmol). The reaction mixture was stirred overnight. The solvent was removed under reduce pressure. Purification of the crude product by flash chromatography on basic alumina (CH_2Cl_2/EtOH 85:15) afforded a pale yellow powder (0.23 g, 60%). ^{31}P NMR (121.49 MHz, D_2O) δ 17.81.^{1}H NMR (300.13 MHz) δ 6.91 (1H, d, *J* = 3.02), 4.78–4.67 (2H, m), 4.59–4.53 (1H, m), 4.41–4.35 (1H, m), 3.87–3.69 (2H, m), 3.65–3.57 (2H, m), 2.78–2.52 (3H, m), 1.64 (3H, d, *J* = 14), 1.35–1.27 (12H, m). ^{13}C NMR (75.47 MHz) δ 161.5 ($1C^{IV}$, s), 158.5 (1C, s), 144.7 (1C, d, *J* = 8.0), 76.6 ($1C^{IV}$, d, *J* = 153.74Hz), 75.7 (1C, d, *J* = 8.0), 75.58 (1C, d, *J* = 8.0), 61.8 (1C, d, *J* = 3.5), 49.1 (1C, d, *J* = 2.3), 43.4 (2C, s), 31.7 (1C, s), 24.1 (1C, d, *J* = 3.4), 23.9 (1C, d, *J* = 3.4), 23.7 (1C, d, *J* = 5.2), 23.5 (1C, d, *J* = 5.2), 19.89 (1C, d, *J* = 1.7). ESI-MS/MS : $[M+H^+]$: 422.22.

Synthesis of the nitrone Agm-DIPPMPO 12

Agm-DIPPMPO 12: To a mixture of agmantine (0,21 g, 0,84 mmol) in acetonitrile (5 mL) was added NHS-DIPPMPO (0.28 g, 0.64 mmol) in 8 mL of anhydrous acetonitrile followed by the addition of N-ethyldiisopropylamine (0.33 mL, 1.94 mmol). The reaction mixture was stirred overnight. The solvent was removed under reduce pressure. Purification of the crude product by flash chromatography on basic alumina (CH_2Cl_2/EtOH 75:25) afforded a pale yellow powder (0.277 g, 95%). ^{31}P NMR (121.49 MHz, D_2O) δ 18.88. ^{1}H NMR (300.13 MHz) δ 7,36 (1H, d, *J* = 2.8), 4.85–4.75 (2H, m), 4.36–4.29 (1H, m), 4.20–4.14 (1H, m), 3.14–3.05 (4H, m), 2.98–2.60 (3H, m), 1.67 (3H, d, *J* = 14.9), 1.60–1.50 (4H, m), 1.31–1.26 (12H, m). ^{13}C NMR (75.47 MHz) δ 162.9 ($1C^{IV}$, s), 158.9 (1C, s), 144.3 (1C,d, *J* = 7.5), 77.3 ($1C^{IV}$, d, *J* = 153.7), 75.6 (1C, d, *J* = 7.5), 75.39 (1C, d, *J* = 8.0), 64.6 (1C, d, *J* = 2.8), 46.2 (1C, d, *J* = 2.3), 41.51 (1C, s), 40.6 (1C, s), 30.7 (1C, s), 26.9 (1C, s), 26.0 (1C, s), 24.1 (1C, d, *J* = 2.9), 24.0 (1C, d, *J* = 4.0), 23.7 (1C, d, J = 6.9), 23.6 (1C, d, *J* = 4.6), 19.99 (1C, s). ESI-MS/MS : $[M+H^+]$: 450.25.

Mitochondrial uptake studies

Mitochondria were isolated from rat heart as described by Sethumadhavan S. et al.[45] Briefly, freshly isolated heart tissue was homogenized in modified Chappell Perry medium: 10 mM HEPES, 100 mM KCl, 1 mM EGTA, 5 mM $MgSO_4$, 1 mM ATP, and 0.2% BSA, pH 7.4. Homogenates were centrifuged at 700 × *g* for 15 min at 4°C. The supernatant was transferred to a cold clean tube and subjected to a high speed centrifugation (10,000 × *g*, 15 min, 4°C). The final supernatant was discarded, and the mitochondrial pellet was washed twice. Finally, the pellets were resuspended in storage buffer: 10 mM HEPES, 100 mM KCl, and 1 mM EGTA, pH 7.4. Mitochondrial protein was quantified by bicinchoninic acid method and used immediately for uptake assays. Incubations were performed in 10 mM HEPES buffer (pH = 7.2) containing KCl (120 mM), EGTA (1 mM), succinate (5 mM) with 10μM of the spin trap solution. Aliquots of the supernatant were collected at 0 and 30 min of incubation for HPLC analysis. Aliquots of the initial solutions and samples at time 0 and 30

min were analyzed, and the initial reagent solution after 30 min was also re-injected to confirm the stability of the compounds tested over the course of experiment.

After incubation, the mixtures were centrifugated (10 min x 1,000g, 4°C) and supernatant was analyzed by HPLC with UV-Vis absorption detection.

Supplementary Material

Refer to Web version on PubMed Central for supplementary material.

Acknowledgments

A. R. thanks the Hungarian Science Fund for partial funding of this work (grant OTKA T-046953). The authors thank Patrick Bernasconi (Aix-Marseille University) for EPR technical support and F. Peyrot, J.-L. Boucher and Y. M. Frapart for discussions.

Funding Sources. This work was supported by Aix-Marseille University, CNRS and by "Agence Nationale de la Recherche" (ANR-09-BLAN-0193-02, SPIN BioRad).

Abbreviations

DEPMPO	5-(diethoxyphosphoryl)-5-methyl-pyrroline N-oxide
DIPPMPO	5-(diisopropyloxyphosphoryl)-5-methyl-pyrroline N-oxide
DMPO	5,5-dimethyl-pyrroline N-oxide
NHS-DIPPMPO	(N-hydroxysuccinimidyl-DIPPMPO)
EMPO	5-ethoxycarbonyl-5-methyl-pyrroline N-oxide
HX	hypoxanthine
Mito-DIPPMPO	(4R*, 5R*) 5-(diisopropyloxyphosphoryl)-5-methyl-4-[({[2-(triphenylphosphonio)-ethyl]carbamoyl}oxy)methyl]pyrroline N-oxide bromide
$Mito_{10}$-DEPMPO	(4R*, 5R*) 5-(diethoxyphosphoryl)-5-methyl-4-[({[2-(triphenylphosphonio)-decyl]carbamoyl}oxy)methyl]pyrroline N-oxide bromide
$Mito_5$-DIPPMPO	(4R*, 5R*) 5-(diisopropyloxyphosphoryl)-5-methyl-4-[({[2-(triphenylphosphonio)-pentyl]carbamoyl}oxy)methyl]pyrroline N-oxide bromide
Mito-bis-DIPPMPO	(4R*, 5R*) 5-(diisopropyloxyphosphoryl)-5-methyl-4-[({bis [2-(triphenylphosphonio)-ethyl]carbamoyl}oxy)methyl]pyrroline N-oxide bromide
TrA-DEPMPO	5-(diethoxyphosphoryl)-5-methyl-4-[({trityl-2-aza-ethyl}-carbamoyl)-oxy-methyl]pyrroline N-oxide

Gua-DIPPMPO	5-(diisopropyloxyphosphoryl)-5-methyl-4-[({[2-(guanidino)-ethyl] carbamoyl}oxy)methyl]-5-methyl-1-pyrroline N-oxide
Agm-DIPPMPO	5-(diisopropyloxyphosphoryl)-5-methyl-4-[({[2-(guanidino)-buthyl] carbamoyl}oxy)methyl]-5-methyl-1-pyrroline N-oxide
SOD	superoxide dismutase
XO	xanthine oxidase
ROS	reactive oxygen species
RNS	reactive nitrogen species

References

1. Pryor WA, Houk KN, Foote CS, Fukuto JM, Ignarro LJ, Squadrito GL, Davies KJA. Free radical biology and medicine: it's a gas, man! Am J Physiol-Reg I. 2006; 291:R491–R511.
2. Floyd RA. Serendipitous findings while researching oxygen free radicals. Free Radic Biol Med. 2009; 46:1004–1013. [PubMed: 19439210]
3. Halliwell, B., Gutteridge, JMC. Free Radicals in Biology And Medicine. 4. Cary, North Carolina, U.S.A: Oxford Univ Pr; 2007.
4. Hadfield KA, Pattison DI, Brown BE, Hou LM, Rye KA, Davies MJ, Hawkins CL. Myeloperoxidase-derived oxidants modify apolipoprotein A-I and generate dysfunctional high-density lipoproteins: comparison of hypothiocyanous acid (HOSCN) with hypochlorous acid (HOCI). Biochem J. 2013; 449:531–542. [PubMed: 23088652]
5. Vasquez-Vivar J. Tetrahydrobiopterin, superoxide, and vascular dysfunction. Free Radic Biol Med. 2009; 47:1108–1119. [PubMed: 19628033]
6. Wright RM, McManaman JL, Repine JE. Alcohol-induced breast cancer: a proposed mechanism. Free Radic Biol Med. 1999; 26:348–354. [PubMed: 9895226]
7. Lin MT, Beal MF. Mitochondrial dysfunction and oxidative stress in neurodegenerative diseases. Nature. 2006; 443:787–795. [PubMed: 17051205]
8. Schriner SE, Linford NJ, Martin GM, Treuting P, Ogburn CE, Emond M, Coskun PE, Ladiges W, Wolf N, Van Remmen H, Wallace DC, Rabinovitch PS. Extension of murine life span by overexpression of catalase targeted to mitochondria. Science. 2005; 308:1909–1911. [PubMed: 15879174]
9. Zielonka J, Zielonka M, Sikora A, Adamus J, Joseph J, Hardy M, Ouari O, Dranka BP, Kalyanaraman B. Global profiling of reactive oxygen and nitrogen species in biological systems. J Biol Chem. 2012; 287:2984–2995. [PubMed: 22139901]
10. Wardman P. Fluorescent and luminescent probes for measurement of oxidative and nitrosative species in cells and tissues: progress, pitfalls, and prospects. Free Radic Biol Med. 2007; 43:995–1022. [PubMed: 17761297]
11. Vasquez-Vivar J, Kalyanaraman B, Martasek P, Hogg N, Masters BSS, Karoui H, Tordo P, Pritchard KA. Superoxide generation by endothelial nitric oxide synthase: the influence of cofactors. P Natl Acad Sci USA. 1998; 95:9220–9225.
12. Buettner GR, Mason RP. Spin-trapping methods for detecting superoxide and hydroxyl free-radicals in-vitro and in-vivo. Methods in Enzymology. 1990; 186:127–133. [PubMed: 2172700]
13. Velayutham M, Hemann C, Zweier JL. Removal of H_2O_2 and generation of superoxide radical: role of cytochrome c and NADH. Free Radic Biol Med. 2011; 51:160–170. [PubMed: 21545835]

14. Mitchell DG, Rosen GM, Tseitlin M, Symmes B, Eaton SS, Eaton GR. Use of rapid-scan EPR to improve detection sensitivity for spin-trapped radicals. Biophys J. 2013; 105:338–342. [PubMed: 23870255]
15. Hawkins CL, Davies MJ. Detection and characterisation of radicals in biological materials using EPR methodology. Biochim Biophys Acta. 2013; 840:708–721.
16. Hardy M, Chalier F, Ouari O, Finet JP, Rockenbauer A, Kalyanaraman B, Tordo P. Mito-DEPMPO synthesized from a novel NH2-reactive DEPMPO spin trap: a new and improved trap for the detection of superoxide. Chem Commun. 2007; (10):1083–1085.
17. Frejaville C, Karoui H, Tuccio B, Lemoigne F, Culcasi M, Pietri S, Lauricella R, Tordo P. 5-(Diethoxyphosphoryl)-5-methyl-1-pyrroline N-oxide - a new efficient phosphorylated nitrone for the in-vitro and in-vivo spin-trapping of oxygen-centered radicals. J Med Chem. 1995; 38:258–265. [PubMed: 7830268]
18. Olive G, Mercier A, Le Moigne F, Rockenbauer A, Tordo P. 2-Ethoxycarbonyl-2-methyl-3,4-dihydro-2H-pyrrole-1-oxide: evaluation of the spin trapping properties. Free Radic Biol Med. 2000; 28:403–408. [PubMed: 10699752]
19. Kim SU, Liu Y, Nash KM, Zweier JL, Rockenbauer A, Villamena FA. Fast reactivity of a cyclic nitrone-calix[4]pyrrole conjugate with superoxide radical anion: theoretical and experimental studies. J Am Chem Soc. 2010; 132:17157–17173. [PubMed: 21070040]
20. Villamena F, Gallucci J, Velayutham M, Hadad C, Zweier J. Spin trapping by 5-carbamoyl-5-methyl-1-pyrroline N-oxide (AMPO): theoretical and experimental studies. Free Radic Biol Med. 2003; 35:S15–S15.
21. Finkelstein E, Rosen GM, Rauckman EJ. Spin trapping - kinetics of the reaction of superoxide and hydroxyl radicals with nitrones. J Am Chem Soc. 1980; 102:4994–4999.
22. Finkelstein E, Rosen GM, Rauckman EJ. Production of hydroxyl radical by decomposition of superoxide spin-trapped adducts. Mol Pharmacol. 1982; 21:262–265. [PubMed: 6285165]
23. Hardy M, Bardelang D, Karoui H, Rockenbauer A, Finet JP, Jicsinszky L, Rosas R, Ouari O, Tordo P. Improving the trapping of superoxide radical with a beta-cyclodextrin-5-diethoxyphosphoryl-5-methyl-1-pyrroline-N-oxide (DEPMPO) conjugate. Chemistry-a European Journal. 2009; 15:11114–11118.
24. Smith RAJ, Hartley RC, Murphy MP. Mitochondria-targeted small molecule therapeutics and probes. Antioxid Redox Sign. 2011; 15:3021–3038.
25. Hoye AT, Davoren JE, Wipf P, Fink MP, Kagan VE. Targeting mitochondria. Acc Chem Res. 2008; 41:87–97. [PubMed: 18193822]
26. Sheu SS, Nauduri D, Anders MW. Targeting antioxidants to mitochondria: a new therapeutic direction. Bba-Mol Basis Dis. 2006; 1762:256–265.
27. Szewczyk A, Wojtczak L. Mitochondria as a pharmacological target. Pharmacol Rev. 2002; 54:101–127. [PubMed: 11870261]
28. Smith RAJ, Porteous CM, Coulter CV, Murphy MP. Selective targeting of an antioxidant to mitochondria. Eur J Biochem. 1999; 263:709–716. [PubMed: 10469134]
29. Robertson L, Hartley RC. Synthesis of N-arylpyridinium salts bearing a nitrone spin trap as potential mitochondria-targeted antioxidants. Tetrahedron. 2009; 65:5284–5292. [PubMed: 19693262]
30. James AM, Cocheme HM, Smith RAJ, Murphy MP. Interactions of mitochondria-targeted and untargeted ubiquinones with the mitochondrial respiratory chain and reactive oxygen species - Implications for the use of exogenous ubiquinones as therapies and experimental tools. J Biol Chem. 2005; 280:21295–21312. [PubMed: 15788391]
31. Adlam VJ, Harrison JC, Porteous CM, James AM, Smith RAJ, Murphy MP, Sammut IA. Targeting an antioxidant to mitochondria decreases cardiac ischemia-reperfusion injury. Faseb J. 2005; 19:1088–1095. [PubMed: 15985532]
32. Xu YK, Kalyanaraman B. Synthesis and ESR studies of a novel cyclic nitrone spin trap attached to a phosphonium group-a suitable trap for mitochondria-generated ROS? Free Radical Res. 2007; 41:1–7. [PubMed: 17164173]
33. Quin C, Trnka J, Hay A, Murphy MP, Hartley RC. Synthesis of a mitochondria-targeted spin trap using a novel Parham-type cyclization. Tetrahedron. 2009; 65:8154–8160. [PubMed: 19888470]

34. Hardy M, Rockenbauer A, Vasquez-Vivar J, Felix C, Lopez M, Srinivasan S, Avadhani N, Tordo P, Kalyanaraman B. Detection, characterization, and decay kinetics of ROS and thiyl adducts of Mito-DEPMPO spin trap. Chem Res Toxicol. 2007; 20:1053–1060. [PubMed: 17559235]
35. Rockenbauer A, Korecz L. Automatic computer simulations of ESR spectra. Appl Magn Reson. 1996; 10:29–43.
36. Clement JL, Ferre N, Siri D, Karoui H, Rockenbauer A, Tordo P. Assignment of the EPR spectrum of 5,5-dimethyl-1-pyrroline N-oxide (DMPO) superoxide spin adduct. J Org Chem. 2005; 70:1198–1203. [PubMed: 15704951]
37. Rockenbauer A, Clement JL, Culcasi M, Mercier A, Tordo P, Pietri S. Combined ESR and thermodynamic studies of the superoxide adduct of 5-(diethoxyphosphoryl)-5-methyl-1-oyrroline N-oxide (DEPMPO): hindered rotation around the O-O bond evidenced by two-dimensional simulation of temperature-dependent spectra. J Phys Chem A. 2007; 111:4950–4957. [PubMed: 17518450]
38. Houriez C, Ferre N, Siri D, Tordo P, Masella M. Structure and spectromagnetic properties of the superoxide radical adduct of DMPO in water: elucidation by theoretical investigations. J Phys Chem B. 2010; 114:11793–11803. and references cited herein. [PubMed: 20722404]
39. Hausladen A, Fridovich I. Competitive-inhibition of xanthine-oxidase by guanidinium - dependence upon monovalent anions and effects on production of superoxide. Arch Biochem Biophys. 1993; 304:479–482. [PubMed: 8394058]
40. Ross MF, Da Ros T, Blaikie FH, Prime TA, Porteous CM, Severina II, Skulachev VP, Kjaergaard HG, Smith RAJ, Murphy MP. Accumulation of lipophilic dications by mitochondria and cells. Biochem J. 2006; 400:199–208. [PubMed: 16948637]
41. Hardy M, Chalier F, Ouari O, Finet JP, Rockenbauer A, Kalyanaraman B, Tordo P. Mito-DEPMPO synthesized from a novel NH_2 -reactive DEPMPO spin trap: a new and improved trap for the detection of superoxide. Chem Commun. 2007:1083–1085.
42. Zon J. Synthesis of diisopropyl 1-nitroalkanephosphonates from diisopropyl 1-oxoalkanephosphonate. Synthesis. 1984; 8:661–663.
43. Li, S., Zhou, X., Wang, L., Xu, C., Ruan, C., Lin, C., Xiao, J., Zheng, Z., Liu, H., Xie, Y., Zhong, W., Cui, H. Preparation of tyrosine derivs. substituted by alkanoyl as hPPARα and & hPPARγ agonists. PCT Int Appl. WO2005116018 (A1). 2005.
44. McAllister PR, Dotson MJ, Grim SO, Hillman GR. Effects of phosphonium compounds on schistosoma mansoni. J Med Chem. 1980; 23:862–865. [PubMed: 7401115]
45. Sethumadhavan S, Vasquez-Vivar J, Migrino RQ, Harmann L, Jacob HJ, Lazar J. Mitochondrial DNA variant for complex I reveals a role in diabetic cardiac remodeling. J Biol Chem. 2012; 287:22174–22182. [PubMed: 22544750]

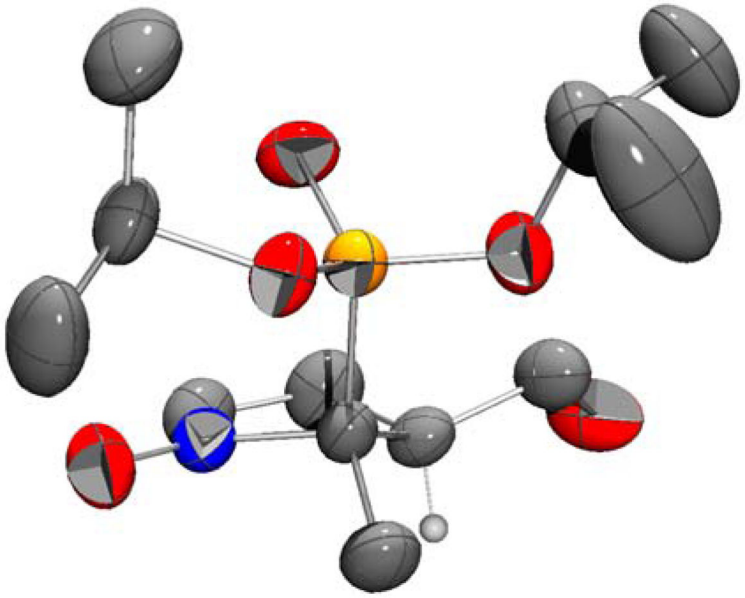

Figure 1.
Geometry of compound **4** from X-ray diffraction analysis (Pov-Ray view)

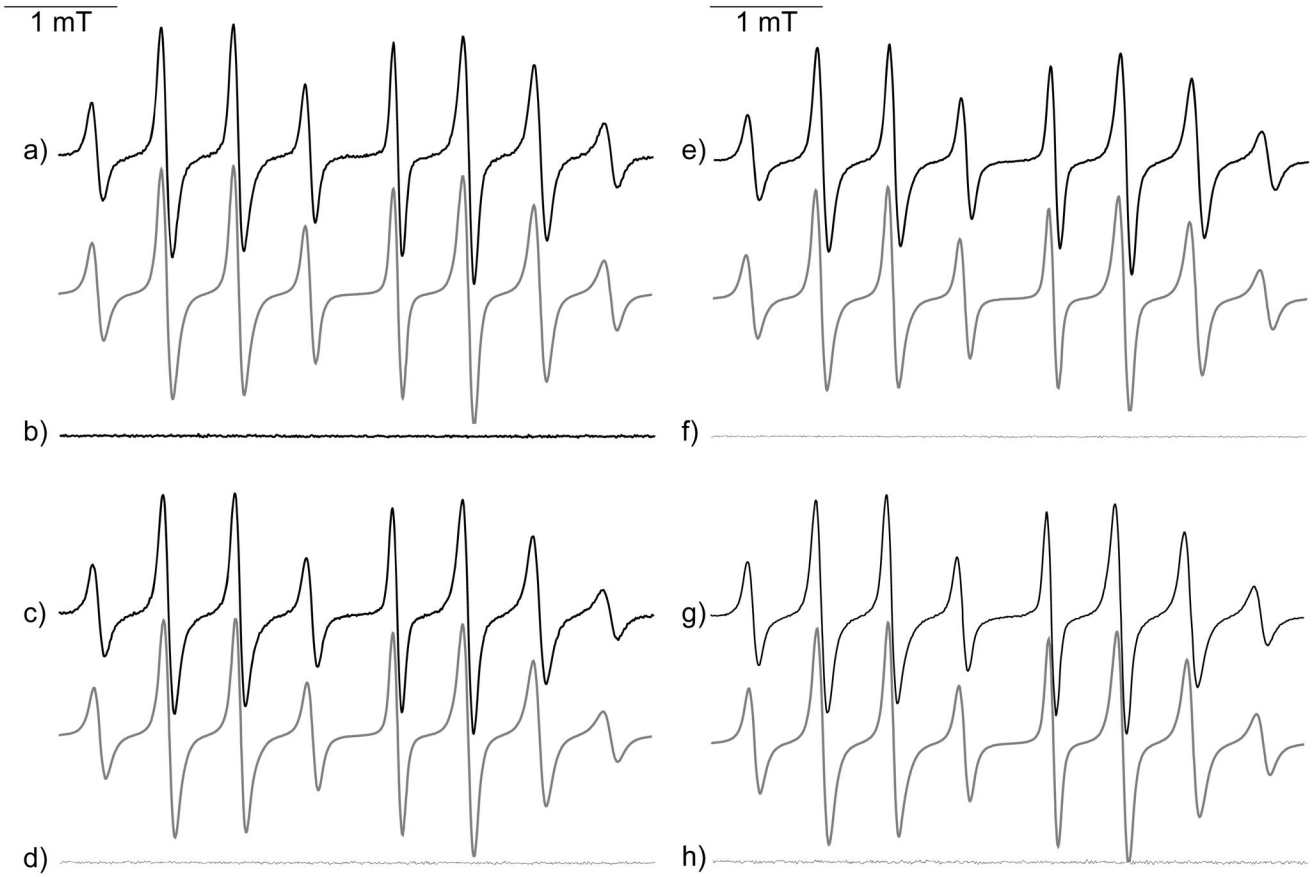

Figure 2. Spin trapping of superoxide radical using Mito-DIPPMPO (6), Mito-bis-DIPPMPO (7), $Mito_5$-DIPPMPO (8), $Mito_{10}$-DEPMPO (9)

(a) EPR spectrum obtained after 10 min incubation of a mixture containing hypoxanthine (HX) (0.4 mM), xanthine oxidase (XO) (0.04 U mL^{-1}), DTPA (1 mM) and **6** (20 mM) in oxygen-bubbled phosphate buffer (0.1 M, pH 7.3); (b) As in (a) but in the presence of SOD (600 U mL^{-1}). (c) As in (a) but containing **7** (20 mM). (d) As in (c) but in the presence of SOD (600 U mL^{-1}). (e) As in (a) but containing **8** (20 mM). (f) As in (e) but in the presence of SOD (600 U mL^{-1}). (g) As in (a) but containing **9** (20 mM) and 20% DMSO. (h) As in (g) but in the presence of SOD (600 U mL^{-1}). Grey lines: calculated spectra (Table 1). Spectrometer settings: microwave power, 10 mW (a–h); modulation amplitude, 0.7 G (a–h); smooth point, 1 (a–h); gain 75 dB (a–h); sweep time, 41.94 s (a–h); conversion time, 40.96 ms (a–h).

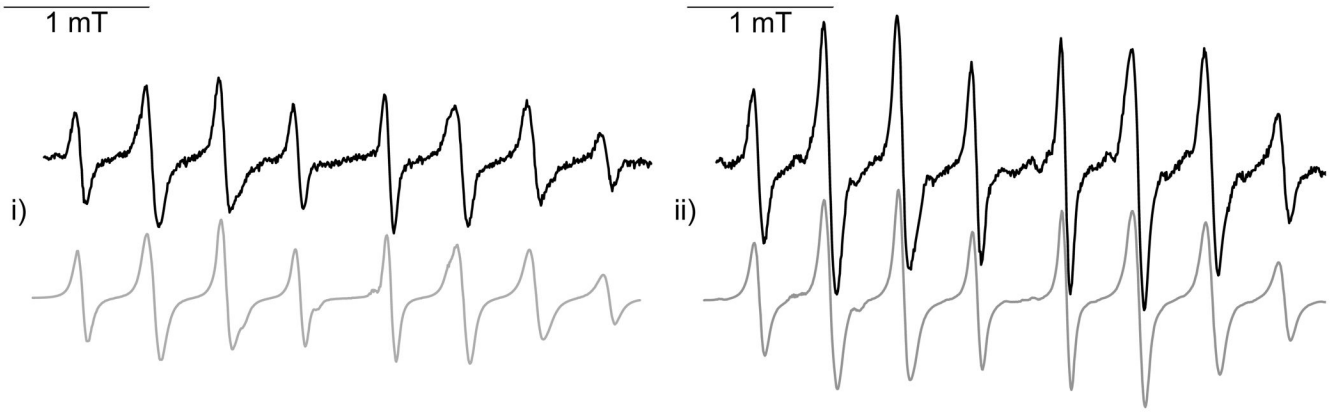

Figure 3. Spin trapping of superoxide radical using Gua-DIPPMPO 11 and Agm-DIPPMPO 12

(i) EPR spectrum obtained after 2 min incubation of a mixture containing the KO_2/CE/DMSO (5 mM/5 mM/5% respectively) system and **12** (25 mM) in a phosphate buffer (0.1 M, pH 7.3). (ii) As in (i) but with **11** (50 mM). Grey lines: calculated spectra (Table 1). Spectrometer settings: microwave power, 10 mW; modulation amplitude, 0.7 G; time constant, 1.28 ms; gain 10^5; sweep time, 21 s; conversion time, 20.48 ms.

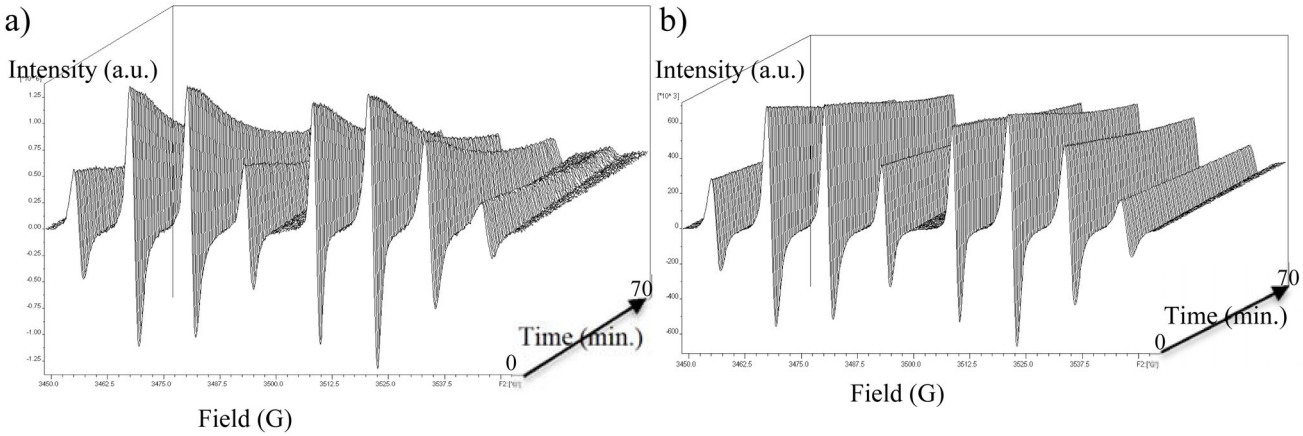

Figure 4.

Kinetics of decay of Mito-bis-DIPPMPO-OOH (**8**-OOH, a) and Mito-DIPPMPO-OOH (**6**-OOH, b)

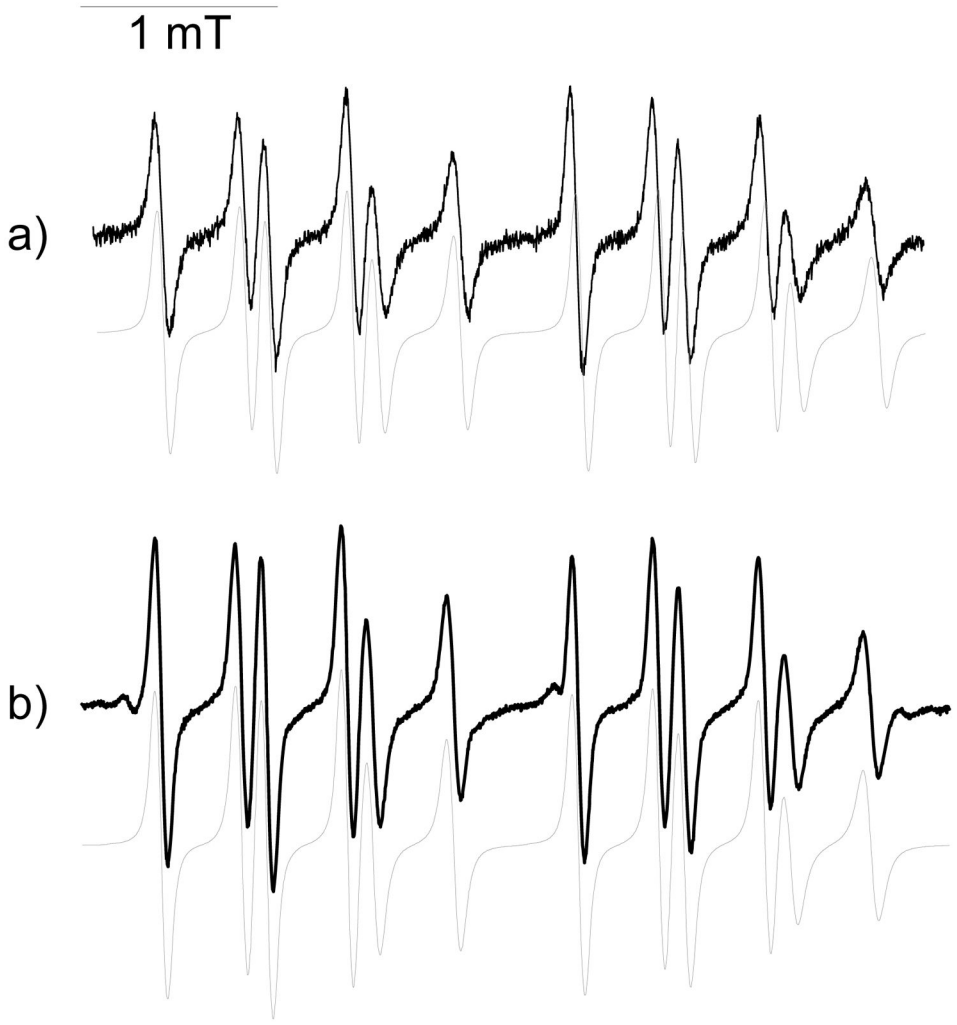

Figure 5. EPR spectra of radical adducts of Mito-bis-DIPPMPO (8) and Mito$_{10}$-DEPMPO (9)

(a) EPR spectrum obtained 10 min after reduction of the **8**-OOH (a) and **9**-OOH (b) adducts (Figure 2) by adding GPx (10 U mL^{-1}) and GSH (1.2 mM) to the incubation mixture and bubbling argon gas for two min. Grey lines: calculated spectra (Table 3). Spectrometers settings: microwave power 30 mW ; modulation amplitude, 0.7; time constant, 1.28 ms; gain 10^5; sweep time, 20.4 ms; conversion time, 41.9.

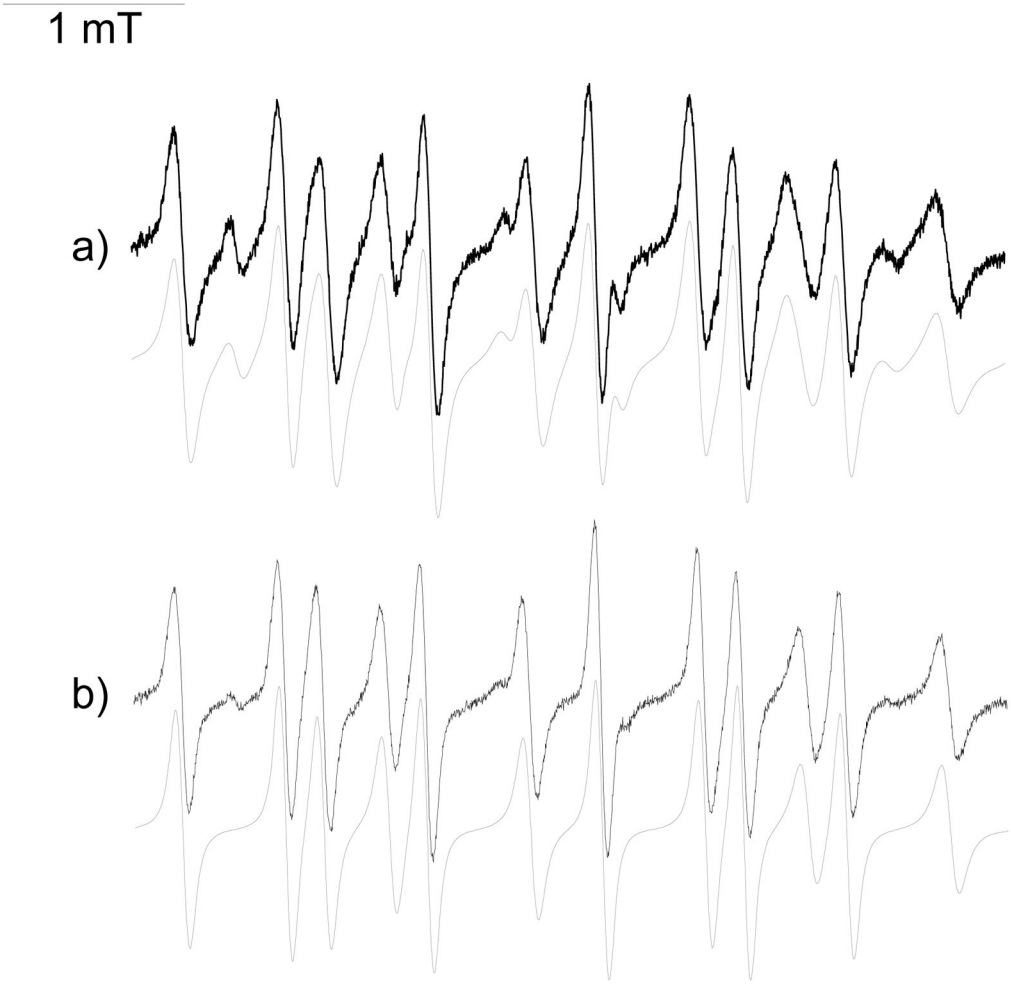

Figure 6. Spin trapping of carbon-centered radical by Mito-bis-DIPPMPO (8) and Mito$_{10}$-DEPMPO (9)

(a) Signal obtained after 15 min incubation of a mixture containing Mito-bis-DIPPMPO (20 mM), H_2O_2 (2 mM), $FeSO_4$ (2 mM), EtOH (15%), DTPA (1 mM) in phosphate buffer (0.1 M, pH 7.3); (b) Signal obtained after 1 min incubation of a mixture containing Mito$_{10}$-DEPMPO (20 mM), H_2O_2 (2 mM), $FeSO_4$ (2 mM), EtOH (15%), DTPA (1 mM) in phosphate buffer (0.1 M, pH 7.3). Grey lines: calculated spectra (Table 3). Spectrometers settings: microwave power 30 mW (a–b); modulation amplitude, 0.7 (a–b); time constant, 1.28 ms (a–b); gain 10^5 (a–b); sweep time, 20.4 ms (a–b); conversion time, 41.9 (a–b).

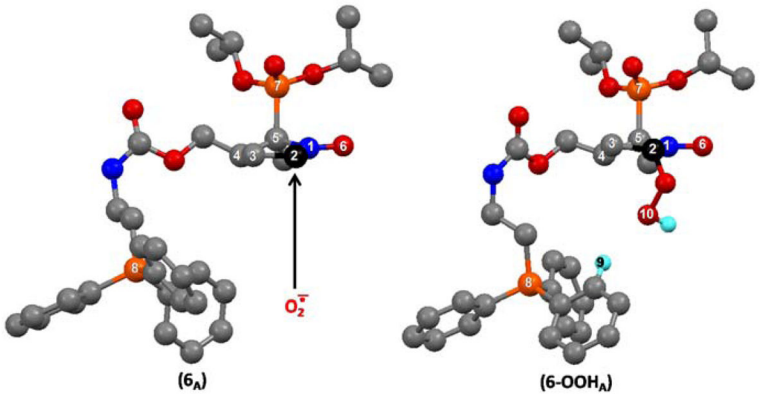

Figure 7.

Calculated DFT [B3LYP 6–31G (d,p), PCM (water)] structures of the lowest energy conformers of Mito-DIPPMPO (**6**$_A$) and Mito-DIPPMPO-OOH (**6**-OOH_A).

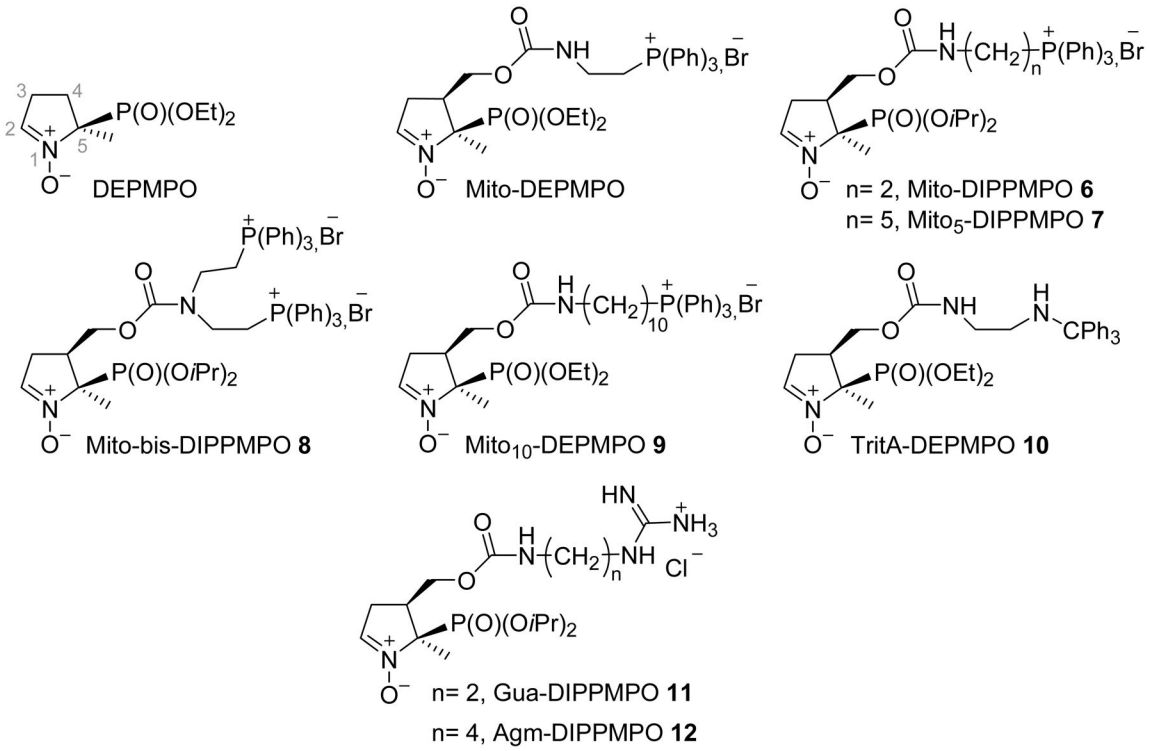

Scheme 1.

Chemical structure of spin traps **6**–**12**.

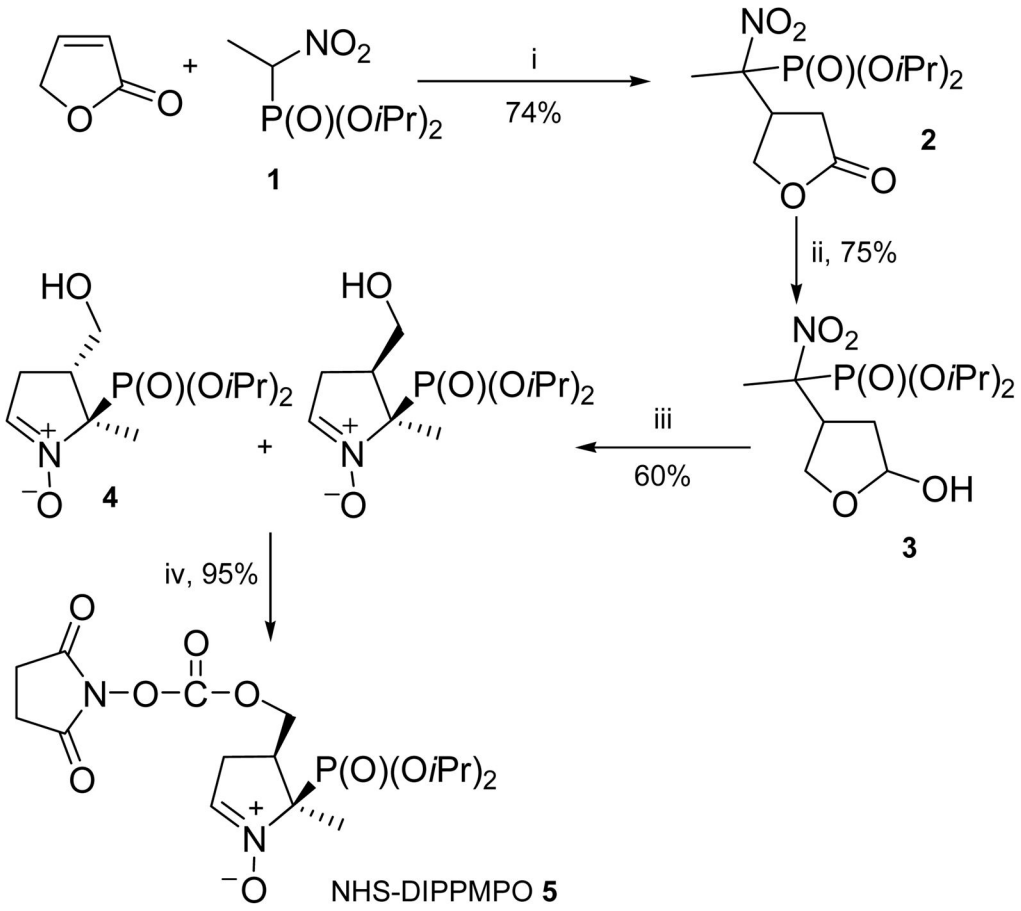

Scheme 2.

Reagents and conditions: i, PBu_3, C_6H_{12}/CH_2Cl_2, rt; ii, DIBAL-H, CH_2Cl_2, −78°C; iii, Zn/NH_4Cl, H_2O/THF, rt; iv, DSC, Et_3N, CH_3CN, rt.

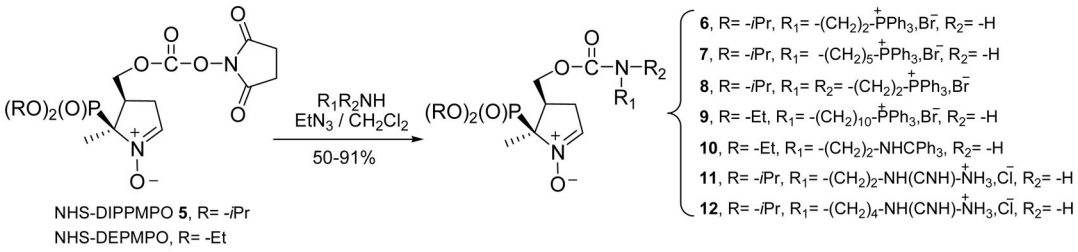

Scheme 3.

Synthesis of compounds **6**–**12**.

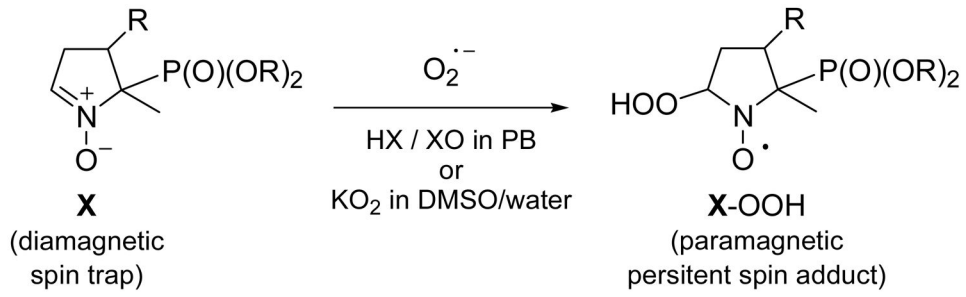

Scheme 4.
Spin trapping experiments

Table 1

Calculated EPR parameters for the superoxide spin adduct of Mito-DEPMPO and newly synthesized nitrones **6–12**.

Spin adduct	Diastereoisomer	Site	k (s^{-1}) *	<a_P>(G)	<a_N>(G)	<$a_{H\beta}$>(G)
Mito-DEPMPO-OOH	*trans (100%)*	T_1 (70%) T_2 (30%)	0.1×10^8	53.27 52.01	12.79 12.97	12.37 10.13
Mito-DIPPMPO-OOH (***6**-OOH*)	„	T_1 (88%) T_2 (12%)	4.2×10^8	53.41 48.05	12.86 12.76	12.13 7.38
Mito-bis-DIPPMPO-OOH (***8**-OOH*)	„	T_1 (54%) T_2 (46%)	2.5×10^8	53.07 45.01	12.83 12.69	12.17 6.06
$Mito_5$-DIPPMPO-OOH (***7**-OOH*)	„	T_1 (60%) T_2 (40%)	5.1×10^8	54.03 51.86	12.80 12.82	12.78 10.57
$Mito_{10}$-DEPMPO-OOH (***9**-OOH*)	„	T_1 (46%) T_2 (54%)	0.67×10^8	54.54 51.48	12.72 12.80	14.66 9.00
Agm-DIPPMPO-OOH (***11**-OOH*)	„	T_1 (79%) T_2 (21%)	0.8×10^7	53.7 51.8	12.8 13.3	11.9 9.5
Gnd-DIPPMPO-OOH (***12**-OOH*)	„	T_1 (74%) T_2 (26%)	0.35×10^7	53.2 51.5	12.8 13.1	12.4 9.4

*Exchange rate constants in s^{-1}. For DMPO-OOH spin adduct a theoretical study in an explicit water solution based on a combined QM/MM/MD protocol showed that the EPR spectrum can be explained in the light of two sites in chemical exchange. Moreover it was demonstrated that each site consists of an equilibrium between the two main 5-membered ring conformations of DMPO ($^3T_4$ and $^4T_3$). For all spin adducts, the *g* values were very close and measured to be 2.006(4).

Table 2

Apparent half-lifetime values for superoxide adducts of DIPPMPO and **6**–**9**, and the ratio values of $t_{1/2}$ **X**-OOH / $t_{1/2}$ DIPPMPO-OOH.

Spin adducts	$t_{1/2}$ (min.)	Ratio
DIPPMPO-OOH	28	1
Mito-DIPPMPO-OOH (6-OOH)	73	2.61
Mito$_5$-DIPPMPO-OOH (7-OOH)	36.6	1.31
Mito-bis-DIPPMPO-OOH (8-OOH)	29.3	1.05
DIPPMPO-OOH[i]	25.5	0.91
Mito$_{10}$-DEPMPO-OOH[i] **(9**-OOH)	22	0.78

[i] in 0.1 M phosphate buffer / DMSO mixture (80:20)

Table 3

EPR parameters of hydroxyl and carbon-centered spin adducts.

Spin adduct	Generating system	a_P (G)	a_N (G)	$a_{H\beta}$ (G)
Mito-bis-DIPPMPO-OH	HX/XO and then GPx/GSH	52.4	13.6	10.5
Mito-bis-DIPPMPO-CH(OH)CH_3	Fe^{2+}, H_2O_2, EtOH (15%)	56.8	14.3	19.8
Mito-DIPPMPO-OH	HX/XO and then GPx/GSH	53.1	13.6	10.5
Mito-DIPPMPO-CH(OH)CH_3	Fe^{2+}, H_2O_2, EtOH (15%)	57.5	14.3	19.7
Mito$_{10}$-DEPMPO-OH	HX/XO and then GPx/GSH	52.9	13.4	10.2
Mito$_{10}$-DEPMPO-CH(OH)CH_3	Fe^{2+}, H_2O_2, EtOH (5%)	57.6	14.2	19.4

Table 4

Percentage of mitochondria uptake determined by HPLC / UV-Vis detection.

Spin traps	Mitochondrial uptake (%)
DIPPMPO	2.4
Mito-DIPPMPO (6)	29
Mito$_5$-DIPPMPO (7)	21.1
Mito$_{10}$-DEPMPO (9)	58
Mito-bis-DIPPMPO (8)	25.6
TritA-DEPMPO (10)	0